

# Voltage-gated Transient Currents in Bovine Adrenal Fasciculata Cells

## II. A-type $K^+$ Current

BORIS MLINAR and JOHN J. ENYEART

From the Department of Pharmacology and the Neuroscience Program, Ohio State University, Columbus, Ohio 43210-1239

**ABSTRACT** In whole cell patch clamp recordings on enzymatically dissociated adrenal zona fasciculata (AZF) cells, a rapidly inactivating A-type  $K^+$  current was observed in each of more than 150 cells. Activation of  $I_A$  was steeply voltage dependent and could be described by a Boltzmann function raised to an integer power of 4, with a midpoint of  $-28.3$  mV. Using the "limiting logarithmic potential sensitivity," the single channel gating charge was estimated to be  $7.2 e$ . Voltage-dependent inactivation could also be described by a Boltzmann function with a midpoint of  $-58.7$  mV and a slope factor of  $5.92$  mV. Gating kinetics of  $I_A$  included both voltage-dependent and -independent transitions in pathways between closed, open, and inactivated states.  $I_A$  activated with voltage-dependent sigmoidal kinetics that could be fit with an  $n^4h$  formalism. The activation time constant,  $\tau_a$ , reached a voltage-independent minimum at potentials positive to  $0$  mV.  $I_A$  currents inactivated with two time constants that were voltage independent at potentials ranging from  $-30$  to  $+45$  mV. At  $+20$  mV,  $\tau_{i(\text{fast})}$  and  $\tau_{i(\text{slow})}$  were  $13.16 \pm 0.64$  and  $62.26 \pm 5.35$  ms ( $n = 34$ ), respectively. In some cells,  $I_A$  inactivation kinetics slowed dramatically after many minutes of whole cell recording. Once activated by depolarization,  $I_A$  channels returned to the closed state along pathways with two voltage-dependent time constants which were  $0.208$  s,  $\tau_{\text{rec-f}}$  and  $10.02$  s,  $\tau_{\text{rec-s}}$  at  $-80$  mV. Approximately 90% of  $I_A$  current recovered with slow kinetics at potentials between  $-60$  and  $-100$  mV.  $I_A$  was blocked by 4-aminopyridine ( $IC_{50} = 629 \mu\text{M}$ ) through a mechanism that was strongly promoted by channel activation. Divalent and trivalent cations including  $Ni^{2+}$  and  $La^{3+}$  also blocked  $I_A$  with  $IC_{50}$ 's of  $467$  and  $26.4 \mu\text{M}$ , respectively. With respect to biophysical properties and pharmacology,  $I_A$  in AZF cells resembles to some extent transient  $K^+$  currents in neurons and muscle, where they function to regulate action potential frequency and duration. The function of this prominent current in steroid hormone secretion by endocrine cells that may not generate action potentials is not yet clear.

Address reprint requests to Dr. John J. Enyeart, Department of Pharmacology, The Ohio State University College of Medicine, Columbus, OH 43210-1239.

## INTRODUCTION

Many cells including secretory cells express multiple  $K^+$  channels which collectively set the membrane potential, determine action potential frequency and duration, and thereby control transmitter and hormone release (Hille, 1992). Although voltage recordings from rat and mouse adrenal zona fasciculata (AZF) cells indicate that the resting potential is determined almost entirely by  $K^+$ , voltage-gated  $K^+$  currents have not been identified or characterized in normal fasciculata cells (Lymangrover, Matthews, and Saffran, 1982; Quinn, Cornwall, and Williams, 1987). The identification and characterization of the  $K^+$  channels expressed by AZF cells will be important to the understanding of the electrical events and ion channels involved in cortisol secretion.

Voltage-gated  $K^+$  channels comprise a diverse set of ion pores distinguishable by their voltage dependence, kinetics, pharmacology, and modulation by neurotransmitters and peptide hormones. Based on their kinetics of inactivation, voltage-gated  $K^+$  channels can be divided into two broad categories: slowly or noninactivating delayed rectifiers, or rapidly inactivating A-type current ( $I_A$ ). Although the general function of  $K^+$  channels is to maintain cells at relatively negative potentials, their great diversity and the expression of multiple  $K^+$  channels by individual cell types indicate a complex role in the regulation of cellular electrical properties. Delayed rectifier  $K^+$  channels generate the repolarizing current of the action potential and limit its duration. Rapidly inactivating  $K^+$  currents were first described in molluscan neurons, where they were found to regulate the action potential spacing controlling the rate of repetitive action potential firing (Connor and Stevens, 1971; Neher, 1971). Since their first description, a spectrum of transient  $K^+$  currents have been described in a variety of invertebrate and vertebrate cells. In vertebrates, A-type currents are present in peripheral and central neurons, smooth muscle, and cardiac cells (Belluzzi, Sacchi, and Wanke, 1985; Clark, Giles, and Imaizumi, 1988; Cooper and Shrier, 1989; Imaizumi, Muraki, and Watanabe, 1990; Fickler and Heinemann, 1992). In addition to spacing action potentials,  $I_A$  may regulate other parameters, including action potential duration in heart cells (Giles and Imaizumi, 1988).

Characterization of the biophysical properties of  $I_A$  in mammalian cells has been hampered by the coexpression of multiple  $K^+$  subtypes by most cells. Multiple currents have been observed in a number of endocrine cells including those of the adrenal glomerulosa (Brauneis, Vassilev, Quinn, Williams, and Tillotson, 1991). However, no comprehensive description of the biophysical properties of  $I_A$  in adrenal cells has been reported. In this study we have identified a rapidly inactivating  $K^+$  current that is prominent in bovine AZF cells. The absence of other  $K^+$  channels subtypes allowed the voltage-dependent gating and kinetics of these currents to be described over a wide range of potentials. Several unusual properties of  $I_A$  not previously described in mammalian cells are reported.

## MATERIALS AND METHODS

Isolation and culture of AZF cells were as described in the accompanying paper (Mlinar, Biagi, and Enyeart, 1993b). Nimodipine was kindly provided by Dr. Alexander Scriabine, Miles Institute of Preclinical Pharmacology (West Haven, CT). GTP, GTP- $\gamma$ -S, MgATP,  $NiCl_2$ ,  $LaCl_3$ ,

tetraethylammonium chloride, and 4-aminopyridine (4-AP) were purchased from Sigma Chemical Co. (St. Louis, MO). Penfluridol was purchased from Janssen Pharmaceutical (Beerse, Belgium).  $\alpha$ -Dendrotoxin was purchased from Alomone Labs (Jerusalem, Israel).

#### *Solutions for Patch Clamp*

For recording whole cell K<sup>+</sup> currents, the standard pipette solution was 120 mM KCl, 10 mM HEPES, 2 mM MgCl<sub>2</sub>, 0.1 mM BAPTA, and 2 mM MgATP with pH buffered to 7.2 using KOH. In some recordings, noted in the text, the pipette solution contained 200  $\mu$ M GTP- $\gamma$ -S. The external solution consisted of 140 mM NaCl, 5 mM KCl, 2 mM CaCl<sub>2</sub>, 2 mM MgCl<sub>2</sub>, 10 mM HEPES, and 5.0 mM glucose with pH titrated to 7.35 using KOH.

#### *Recording Conditions*

Recording conditions were as those described in Mlinar et al. (1993b) with several exceptions. Whole cell K<sup>+</sup> currents were, on the average, 5–10 times larger than Ca<sup>2+</sup> currents in adrenal cells of comparable size. To minimize series resistance errors, smaller cells (15–25 pF) and lower resistance electrodes (<1.5 M $\Omega$ ) were chosen for characterization of biophysical properties. Currents in these cells were not qualitatively different from those in larger cells. Access resistance was estimated from the transient cancellation controls of the patch amplifier. When the product of access resistance and membrane current indicated series resistance errors >3 mV, corrections of membrane potential were made during analysis of records. The combination of access resistance and cell capacitance yielded voltage clamp time constants of  $\sim$ 100  $\mu$ s. Exponential fits and current measurements were made after at least four time constants as determined for individual cells. Voltage-dependent Ca<sup>2+</sup> current through T channels was typically <100 pA with 2 mM Ca<sup>2+</sup> in the bath. T current was blocked by adding 500 nM penfluridol to the perfusate. At this concentration, penfluridol had no effect on voltage-gated K<sup>+</sup> currents.

## RESULTS

In whole cell patch clamp recordings, a rapidly inactivating K<sup>+</sup> current was prominent in each of >100 cells. Fig. 1 shows A-type K<sup>+</sup> currents activated from a holding potential of  $-80$  mV by test potentials ranging from  $-45.1$  to  $+23.4$  mV and the corresponding current–voltage (IV) relationship. Threshold for  $I_A$  activation was approximately  $-40$  mV. In a total of 52 cells,  $I_A$  at  $+20$  mV measured  $2,116 \pm 211$  pA. The magnitude of  $I_A$  was linearly related to cell size as determined from cell capacitance measurements. Peak K<sup>+</sup> current measured at  $+20$  mV was plotted as a function of cell capacitance for the same 52 cells. A least-squares linear regression analysis yielded a line with a slope of  $78.42 \pm 23.24$  pA/pF. When the ratio of current to capacitance was plotted against capacitance, the least-squares linear regression yielded a line with a slope only slightly different from zero ( $-0.365 \pm 1.01$  pA/pF<sup>2</sup>), indicating a nearly constant density of  $I_A$  channels regardless of cell size (data not shown).

#### *Slowing of $I_A$ Inactivation*

When whole cell patch recordings were maintained for periods exceeding 15 min, the rate and extent of  $I_A$  inactivation were occasionally observed to diminish continuously with time. Fig. 2A shows records in which A currents were recorded from a cell during a 31-min period immediately after rupture of the membrane patch. During

the first 10 min of recording, the current was nearly constant and consisted of a largely rapidly inactivating component, which decayed to 1 or 2% of its peak value during a 300-ms depolarizing test pulse. During subsequent minutes, the kinetics of inactivation slowed continuously until after 31 min, and  $I_A$  present at the end of the test pulse had increased from 40 to 1,946 pA. By comparison, the peak current increased from 2,461 to 3,140 pA during this same interval of time.

Fig. 2 *B* shows results from a similar experiment and illustrates the time-dependent increase in both the peak  $I_A$  current (triangles) and the current that remains at the end of the 300-ms depolarizing test pulse. Again, after a delay of ~15 min, the noninactivating component begins to grow until, after 40 min, it has increased 14.5-fold over its initial value. The mechanism that underlies this slowing of

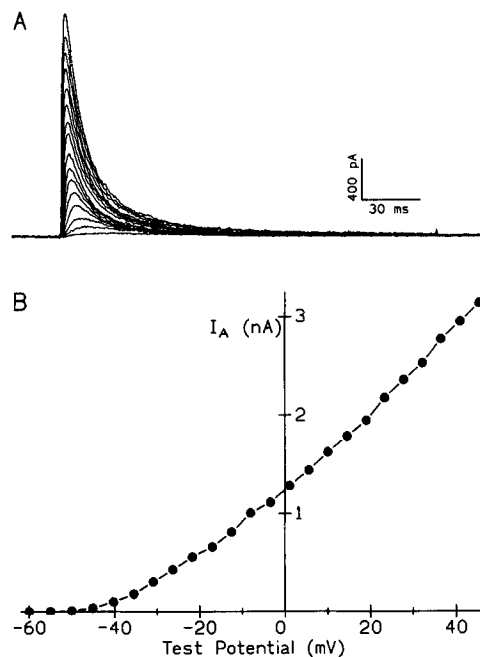


FIGURE 1. A-type  $K^+$  current in bovine AZF cells. Whole cell  $K^+$  currents were activated by voltage steps to various test potentials applied at 30-s intervals from a holding potential of ~80 mV. (A) 16 current traces from a single cell recorded at test potentials between -45.1 and +23.4 mV. (B) IV relationship; peak current amplitudes from same cell are plotted as a function of test potential. Cell 2103#7.

inactivation kinetics subsequent to dialysis of the cytoplasm is unknown. However, it was observed in standard pipette solution and when 200  $\mu$ M GTP- $\gamma$ -S or 500  $\mu$ M GDP- $\beta$ -S were added to the pipette. The noninactivating  $I_A$  retained the same voltage of activation and steady-state inactivation, as well as the same pharmacological sensitivity, as the more typical inactivating current.

In addition to  $I_A$ , a second much smaller (<50 pA)  $K^+$  current with different biophysical and pharmacological properties was initially present in most whole cell recordings from AZF cells. Unlike  $I_A$ , this noninactivating current was insensitive to 4-AP and was available for activation at depolarized holding potentials. With standard pipette solutions, this  $K^+$  current typically grew steadily over many minutes of recording. It was discovered that this novel current could be completely eliminated by

including 200  $\mu\text{M}$  GTP- $\gamma$ -S in the recording pipette (Mlinar, Biagi, and Enyeart, 1993a). In contrast, GTP- $\gamma$ -S had no apparent effect on the biophysical properties of  $I_A$ . By adding GTP- $\gamma$ -S to the pipette solution, we were able to isolate  $I_A$  in AZF cells and characterize its properties without interference from other K<sup>+</sup> channel subtypes.

#### *Voltage-dependent Conductance and Gating*

The instantaneous current-voltage relationship (IIV) or open channel IV provides a measure of the open channel conducting properties of channels. The IIV for  $I_A$  was determined by activating channels with brief (3 ms) depolarizing steps to +50 mV,

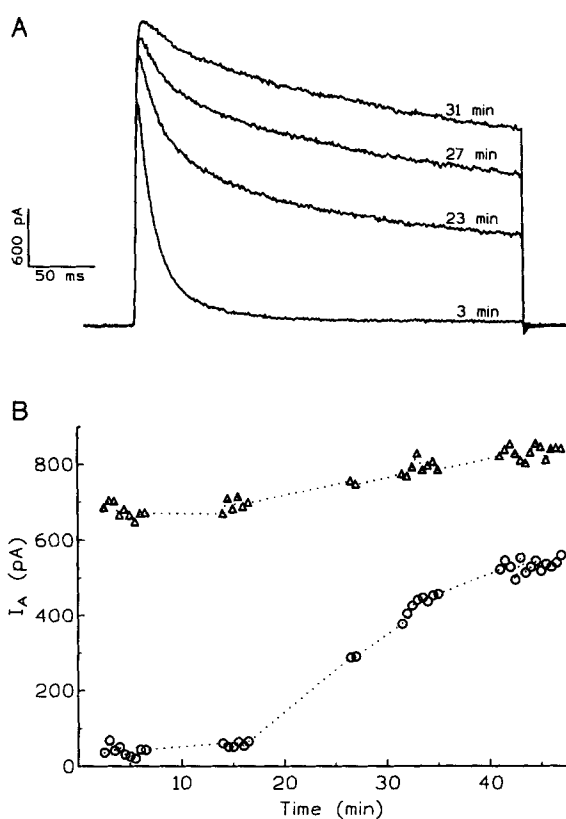


FIGURE 2. Spontaneous slowing of  $I_A$  inactivation kinetics. K<sup>+</sup> currents in AZF cells were activated by 300-ms depolarizing steps to +10 mV applied at 30-s intervals from a holding potential of -80 mV. (A)  $I_A$  current records obtained 3, 23, 27, and 31 min after obtaining whole cell clamp. Cell 2123#4. (B) Plot of peak (triangles) and minimum (circles)  $I_A$  current measured during 300-ms test depolarizations at indicated times. Cell 2123#1.

after which the membrane potential was stepped to new levels between +30 and -110 mV. Current was measured after 1 ms before a significant change in the number of open channels occurred (Fig. 3A). Over a wide range of potentials, the IIV was well fit by the Goldman-Hodgkin-Katz constant field equation. However, at potentials negative to -70 mV,  $I_A$  showed marked rectification and inward K<sup>+</sup> currents were smaller than predicted values (Fig. 3B).

The voltage dependence of  $I_A$  activation was determined by dividing peak current amplitudes taken from the steady-state IV relationship by corresponding amplitudes from the IIVs. These values were then normalized as the fraction of open channels,

plotted against membrane potential, and fit by a Boltzmann function of the form: fraction open =  $1/[1 + \exp(v_{1/2} - v)/K]^N$ , where  $v_{1/2}$  is the voltage where half of the single gate particles are in the "open" conformation,  $K$  is the slope factor, and  $N$  is an integer number of single-gate voltage sensors or conformational states associated with the opening of a single channel. Curves were fit to data points acquired at test potentials between  $-60$  and  $-25$  mV. The activation function was best fit for  $N$  values of 4 or greater (Fig. 4 A, solid line) and had a midpoint at  $-28.3$  mV. The  $M_\infty$  curve

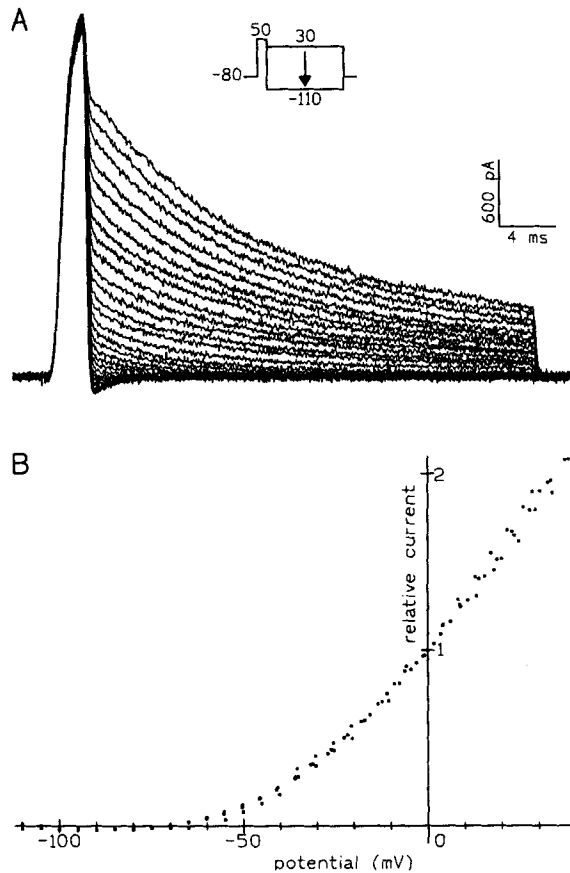


FIGURE 3. Open channel IV relationship for  $I_A$ . After activating  $I_A$  by applying 4-ms test pulses to +50 mV from a holding potential of -80 mV, membrane voltage was stepped to various values between 30 and -100 mV where decaying tail currents were recorded. (A) Tail current records from a single cell. Cell 2103#9. (B) Open channel IV. Maximum tail currents recorded at various potentials were expressed as a fraction of tail current amplitude at 0 mV and plotted against membrane potential. Points are individual plots from four separate cells.

which describes the activation function for one of four single gate voltage sensors has a  $v_{1/2}$  of  $-47.2$  mV and a  $K$  of  $9.6$  mV per  $e$ -fold change (Fig. 4 A, dashed line). These results are consistent with a model in which the opening of a single A-type  $K^+$  channel requires the movement of 9.95 elementary charges through the membrane electric field. By comparison, estimation of the single channel gating charge using the model-independent "limiting logarithmic potential sensitivity" (Almers, 1978; Schoppa, McCormack, Tanouye, and Sigworth, 1992) as described in the accompa-

nying article (Mlinar et al., 1993b) indicated that movements of at least 7.2 unitary charges were associated with the opening of a single A-type K<sup>+</sup> channel (Fig. 4 B).

The voltage-dependent steady-state inactivation of the A-type K<sup>+</sup> current was studied by applying 10-s conditioning pulses to various potentials between -100 and -35 mV, followed by activating voltage steps to +20 mV. The normalized current was

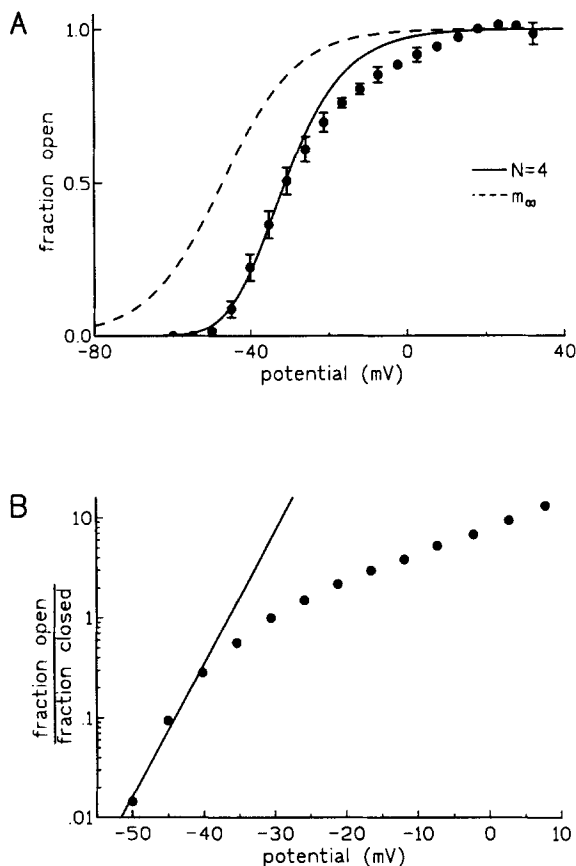


FIGURE 4. Voltage dependence of  $I_A$  current activation and estimate of gating charge. (A) Voltage-dependent activation of  $I_A$  was determined by dividing peak current amplitudes obtained from steady-state IV relationships by corresponding current amplitudes from the open channel IV relationships (see Figs. 1 and 4 for details). These values were then normalized to the maximum permeability. The normalized values representing the fraction of open channels were plotted against membrane potential to give the activation function (values are mean  $\pm$  SEM for five cells). The first seven data points were fit by a Boltzmann expression of the form: fraction open =  $1/[1 + \exp((v_{1/2} - v)/K)]^N$ . Solid line represents activation curve for  $N = 4$ .  $M_\infty$  curve (dashed line) for  $N = 4$  corresponds to activation function of a single gating particle with a  $v_{1/2}$  of -47.2 mV, and a slope factor of 9.6 mV per  $e$ -

fold change. (B) Limiting logarithmic potential sensitivity. The ratio of open to closed A-type K<sup>+</sup> channels was determined from steady-state activation curves from three cells. The logarithm of this ratio was plotted against membrane potential. The limiting slope of this curve computed at potentials between -50 and -40 mV (solid line) correspond to an  $e$ -fold increase per 3.33 mV, or a single channel gating charge of 7.3 elementary charges.

plotted as a function of the conditioning voltage and fitted with the equation:  $I/I_{\max} = 1/[1 + \exp((v - v_{1/2})/K)]$ , where  $I_{\max}$  was the current activated from a holding potential of -90 mV. Inactivation was a steep function of voltage, with  $v_{1/2}$  equal to -58.7 mV and a slope factor  $K$  of 5.92 per  $e$ -fold change (Fig. 5, solid line). Steady-state activation and inactivation curves overlapped slightly at potentials near -45 mV.

## Voltage-dependent Gating Kinetics

The voltage-dependent gating kinetics of  $I_A$ , including activation, inactivation, and recovery from inactivation, were studied over a wide range of potentials. Activation kinetics were voltage dependent and distinguished by sigmoidal onset. For some cells, current traces taken from IV protocols were fit with an equation of the form  $I = I_\infty[1 - \exp(T/\tau_a)]^N \exp(-T/\tau_i)$ , where  $\tau_a$  is the activation time constant,  $\tau_i$  is the inactivation time constant,  $N$  is an integer between 1 and 6, and  $I_\infty$  is the current that would be reached in the absence of inactivation. In other cells, where IVs were

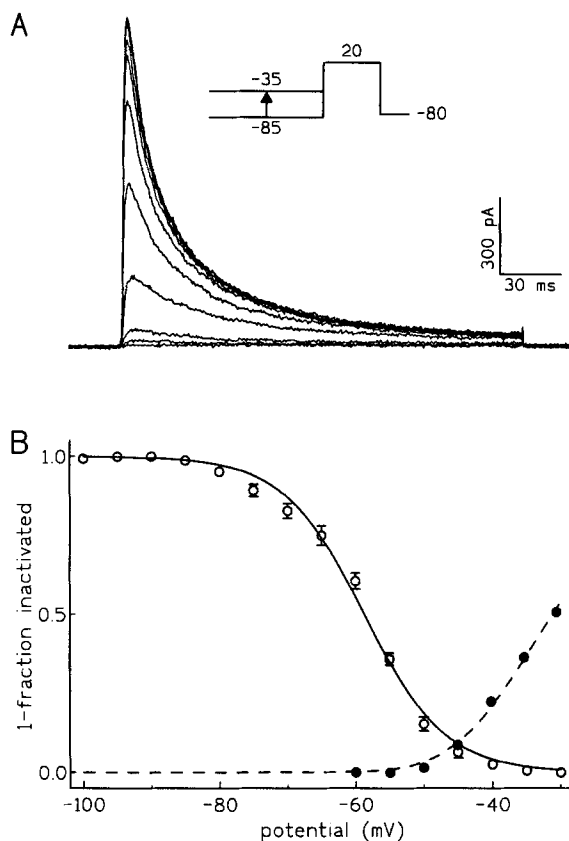


FIGURE 5. Voltage-dependent steady-state inactivation. Inactivation was measured by applying 10-s prepulses to potentials between  $-100$  and  $-35$  mV followed by activating test pulses to  $+20$  mV. (A)  $I_A$  current records showing steady voltage-dependent inactivation at potentials ranging from  $-85$  to  $-35$  mV. Cell 2103#9. (B) Steady-state inactivation curve (solid line). Peak current amplitudes normalized to the maximum current activated from  $-90$  mV were plotted against conditioning voltage. Mean values  $\pm$  SEM ( $n = 5$ ) were fitted to a Boltzmann function of the form:  $I/I_{\max} = 1/[1 + \exp((v - v_{1/2})/K)]$ , where  $v_{1/2} = -58$  mV and  $K = 5.9$  mV. Activation curve (dashed line) is shown for comparison.

recorded only after inactivation had markedly slowed, currents were fit by a simplified version of the equation ignoring inactivation. The activation kinetics of  $I_A$  were voltage dependent and accelerated by stronger depolarizations. Current records in Fig. 6A show  $I_A$  onset kinetics at 14 different test potentials in a cell where inactivation had been allowed to "wash out." A clear sigmoidal onset of A current is present at every potential. Activation kinetics were best fit by  $N$  values of at least 4. For five similar cells, using  $N = 4$ ,  $\tau_a$  varied from 6.72 to 1.27 ms at test potentials of  $-40$  and  $+17$  mV, respectively. The function relating  $\tau_a$  and membrane voltage could



be expressed as a single exponential with an  $e$ -fold change per 14.1 mV and a voltage-independent offset of 1.24 ms (Fig. 6 B).

Rapid inactivation kinetics are a distinctive and defining feature of A-type K<sup>+</sup> currents. The inactivation of  $I_A$  in AZF cells occurred with two distinct time constants, both of which were surprisingly voltage independent over a wide range of potentials. Fig. 7 A shows scaled traces recorded from a single cell at test potentials ranging from -25 to +30 mV. Decaying components of scaled currents were nearly superimposable. For a total of 34 different cells, inactivation measured at +20 mV was described

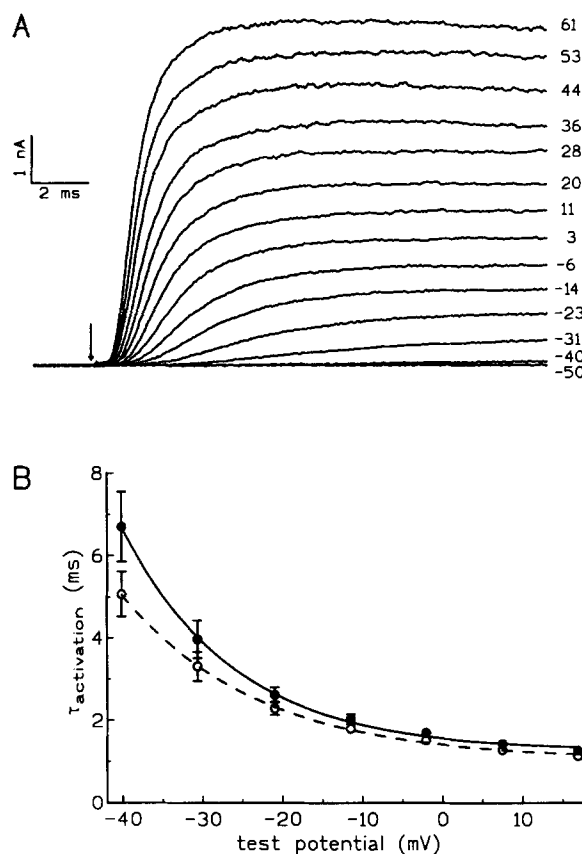


FIGURE 6. Voltage dependence of activation kinetics. Activation time constants were determined in five cells at different test potentials in AZF cells after inactivation had spontaneously washed out. Currents were fit with functions of the form  $I = I_{\max} [1 - \exp(-T/\tau_a)]^N$ , where  $N$  was either 4 or 5. (A) Traces showing noninactivating A currents at 14 different test potential activated by test pulses from -80 mV. Cell 2123#4. (B) Activation time constants were determined by best fits for integer values of  $N = 4$  (filled circles) or 5 (open circles). Relationship between  $\tau_a$  and test voltage was fit by a single exponential with  $e$ -fold change per 14.1 mV and a voltage-independent offset of 1.24 ms. Values are mean  $\pm$  SEM ( $n = 5$ ).

by the sum of two exponentials with time constants of  $13.16 \pm 0.64$  ms ( $\tau_f$ ) and  $62.26 \pm 5.35$  ms ( $\tau_s$ ). Fast and slow time constants did not change for test potentials ranging from -30 to +45 mV. In Fig. 7 B, mean fast and slow time constants determined for five separate cells are plotted against test potential. Least-squares linear regression analysis of these data yielded two lines with slopes not significantly different from zero and intercepts of  $9.66 \pm 0.20$  ms ( $\tau_f$ ) and  $44.97 \pm 0.91$  ms ( $\tau_s$ ). Approximately three-fourths of A current ( $0.77 \pm 0.02$ ,  $n = 34$ ) inactivated via the

fast time constant, and this fraction was constant over the entire range of test voltages (Fig. 7 C).

The kinetics of inactivated A channels returning to the closed state was studied by first clamping cells at  $-20$  mV for 30 s to inactivate  $I_A$ , and then switching to a more negative recovery potential for various periods up to 60 s before applying an activating test pulse to  $+20$  mV. Fig. 8 A illustrates the temporal pattern of A current recovery measured in five cells at  $-70$  and  $-100$  mV. Recovery from inactivation occurred with two time constants, both of which were voltage dependent. Recovery kinetics were studied at five different voltages ranging from  $-70$  to  $-100$  mV. Over

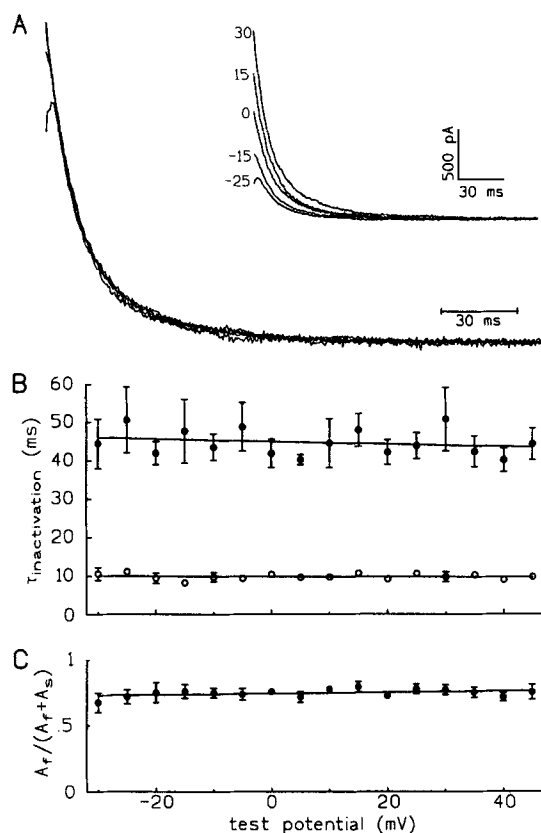


FIGURE 7. Voltage-independent inactivation kinetics.  $I_A$  currents were activated by voltage steps of varying size from a holding potential of  $-90$  mV. Inactivation time constants (slow and fast) were determined at each test potential by fitting the decaying phase of each current with two exponentials. (A) Scaled and unscaled (*inset*) traces recorded at five test potentials. Cell 2103#7. (B) Fast (filled circles) and slow (open circles) inactivation time constants, plotted as a function of test potential. Points are mean  $\pm$  SEM of values from five cells. (C) Fraction of  $I_A$  inactivating with fast time constant at different potentials. After fitting decaying A currents with two exponentials, the fractions inactivating with each time constant were calculated by back extrapolation to  $T = 0$ . Values are mean  $\pm$  SEM of triplicate determinations from five cells.

this range, the fast recovery time constant ( $\tau_{\text{rec-f}}$ ) decreased from 0.61 to 0.04 s, while the slow time constant ( $\tau_{\text{rec-s}}$ ) decreased less dramatically from 17.86 to 8.09 ms (Fig. 8, B and C). The relationships between  $\tau_{\text{rec-f}}$  and membrane voltage could be fit with a single exponential with an  $e$ -fold decrease per 14.2 mV.  $\tau_{\text{rec-s}}$  approached a minimum value of  $\sim 9$  ms at potentials negative to  $-80$  mV. Approximately 90% of inactivated  $I_A$  current recovered with slow kinetics. This fraction was invariant over the range of potentials studied (Fig. 8 D).

Pharmacology of  $I_A$ 

$I_A$  in AZF cells resembled rapidly inactivating  $K^+$  currents in other cells with respect to its sensitivity to organic  $Ca^{2+}$  antagonists.  $I_A$  was blocked by 4-AP and inhibition was promoted by channel opening. The spontaneous disappearance of  $I_A$  inactivation in whole cell recordings allowed the onset of block after channel activation to be clearly observed. Trace 1 in Fig. 9A shows  $I_A$  recorded after inactivation had slowed

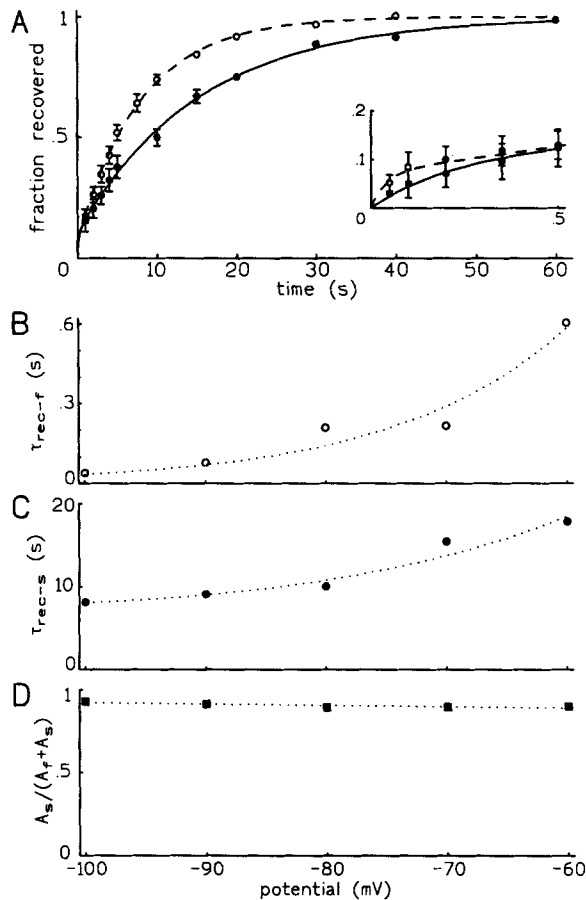


FIGURE 8. Voltage-dependent recovery kinetics of  $I_A$  after inactivation. Time-dependent recovery of  $I_A$  (inactivated by a 30-s prepulse to  $-20$  mV) was monitored at five potentials between  $-60$  and  $-100$  mV by applying voltage steps to  $0$  mV after stepping to recovery potentials for periods ranging from  $0.05$  to  $60$  s. (A) Temporal pattern of  $I_A$  recovery. Peak current amplitudes normalized to maximum current ( $I/I_{max}$ ) are plotted against time at recovery potentials of  $-70$  mV (filled circles) and  $-100$  mV (open circles). Values are mean  $\pm$  SEM ( $n = 5$ ). (Inset) Fractional recovery during first  $0.5$  s. Data points were fit to double exponential functions with fast and slow recovery time constants of  $0.2165$  and  $15.46$  s ( $-70$  mV) and  $0.0398$  and  $8.09$  s ( $-100$  mV). (B and C) Fast ( $\tau_{rec-f}$ ) and slow ( $\tau_{rec-s}$ ) recovery time constants plotted against recovery voltage. Data points are fit with single exponentials corresponding to  $e$ -fold changes

per  $14.18$  mV ( $\tau_{rec-f}$ ) and  $45.24$  mV ( $\tau_{rec-s}$ ). (D) Fraction of  $I_A$  recovering with fast kinetics is plotted against voltage for the same five cells.

dramatically during 30 min of whole cell recording. When a test pulse was applied after superfusing the cell with  $4$  mM 4-AP, block developed rapidly during the course of a  $300$ -ms test depolarization (trace 2). Initially, the current amplitude was reduced by only  $12\%$ . By the end of the depolarizing test pulse, block had reached  $87\%$ . After two additional depolarizations, inhibition reached a steady-state value of nearly  $96\%$  (traces 3 and 4). 4-AP blocked  $I_A$  half-maximally at an estimated concentration of  $629$

$\mu\text{M}$  (Fig. 9 B). By comparison, a second  $\text{K}^+$  channel antagonist, tetraethylammonium (TEA) was much less potent. At a concentration of 10 mM, TEA inhibited  $I_A$  by  $10.8 \pm 4\%$  ( $n = 4$ ). The peptide toxin  $\alpha$ -dendrotoxin potently blocks  $I_A$  in some cells (Halliwell, Othman, Pelchen-Matthews, and Dolly, 1986). At a concentration of 500 nM,  $\alpha$ -dendrotoxin had no effect on AZF  $I_A$  ( $n = 3$ ).

Inorganic divalent and trivalent cations including  $\text{Ni}^{2+}$  and  $\text{La}^{3+}$  also effectively blocked  $I_A$  in AZF cells.  $\text{La}^{3+}$  was the more potent antagonist with an  $\text{IC}_{50}$  of 26.4

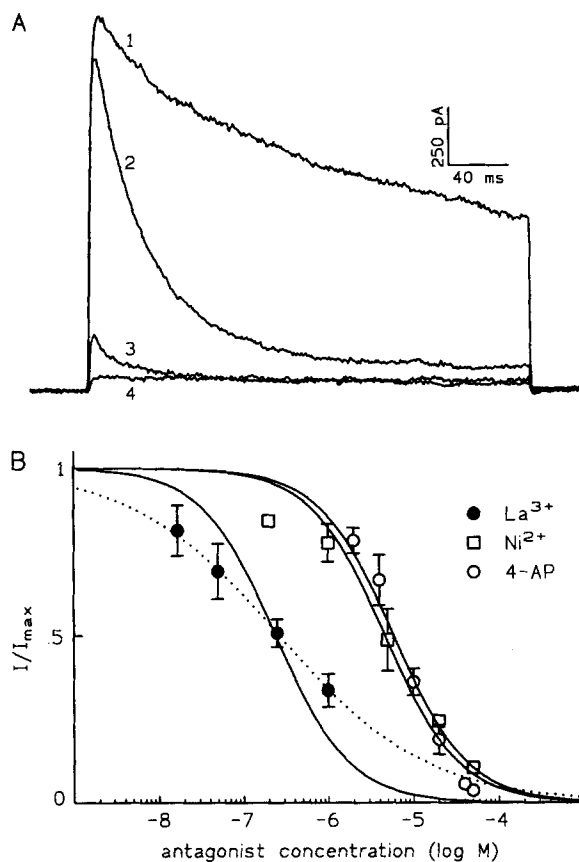


FIGURE 9. Pharmacology of  $I_A$  in AZF cells. Currents were activated by depolarizing steps to +20 mV applied at 30-s intervals from a holding potential of -80 mV. After recording control currents, cells were superfused at 5–6 ml/min with saline containing antagonists. (A) 4-AP. Currents were recorded in control saline for 30 min, at which time inactivation had been largely removed (trace 1). Traces 2, 3, and 4 were recorded 30, 60, and 90 s after superfusion with 4 mM 4-AP. Cell 2103#7. (B) Inhibition curves: After recording currents in control saline, cells were superfused with saline containing  $\text{La}^{3+}$ ,  $\text{Ni}^{2+}$ , or 4-AP at various concentrations. Currents were normalized to maximum current and plotted against antagonist concentration. Inhibition curves were generated by fitting data with an equation of the form  $I/I_{\text{max}} = 1/1 + (B/K_d)^x$ , where  $B$  is the concentration of the blocker,  $K_d$  is the equilibrium dissociation constant, and  $x$  is the Hill coefficient, either 1 (solid line) or  $1/2$  (dashed line).

Values are mean  $\pm$  SEM of three to five determinations.

$\mu\text{M}$ , while  $\text{Ni}^{2+}$  was similar to 4-AP in potency ( $\text{IC}_{50} = 467 \mu\text{M}$ ). The inhibition data for  $\text{La}^{3+}$  were best fit assuming a Hill coefficient of  $1/2$  (dotted line) rather than 1 (solid line).

#### DISCUSSION

In whole cell patch clamp studies we discovered that a rapidly inactivating A-type  $\text{K}^+$  current is uniformly expressed by bovine AZF cells. By including GTP- $\gamma$ -S in the

recording pipette, we were able to study the properties of A-type current without interference from other K<sup>+</sup> channel subtypes. In so doing, we observed some unique kinetic features of this current and uncovered a number of voltage-independent gating transitions which become rate limiting at extreme potentials.

Over a restricted range of test potentials, the voltage-dependent activation of  $I_A$  could be modeled by a Boltzmann function raised to an integer power of at least 4. With stronger depolarizations, the Boltzmann function overestimates the actual fraction of open channels. We have not determined the source of this disparity. The necessity for raising the Boltzmann function to a power of at least 4 in describing the relationship between the membrane voltage and open channel probability indicates that multiple voltage-dependent transitions occur along the pathway from the closed to the open state. A functional  $I_A$  K<sup>+</sup> channel of *Drosophila* muscle consists of four identical subunits (MacKinnon, 1991), which is consistent with the possibility that A channel activation involves the movement of a single independent gating particle associated with each subunit. However, a fourth power relationship between membrane voltage and open probability could also reflect four conformational states of a single channel protein rather than four separate gating particles. Voltage dependence of  $I_A$  activation in several cell types has been fit with Boltzmann functions using  $N$  values of 1 (Belluzzi et al., 1985; Clark et al., 1988; Imaizumi et al., 1990). Comparisons of fits for different integer values of  $N$  are not reported in these studies.

Our estimates of the single channel gating charge made by two separate methods were in reasonable agreement. The estimate using the "limiting logarithmic potential sensitivity" ( $q = 7.2$ ) provides an unrestricted minimum estimate of  $q$  when channels are activated from  $-90$  mV. The slightly larger estimate ( $q = 9.95$ ) obtained using the slope factor of the Boltzmann function is model dependent, but indicative of the steep voltage-dependent activation of  $I_A$  in these cells. The estimates of gating charge that we obtained for  $I_A$  in AZF cells are significantly larger than the values obtained in vertebrate neurons, where values of  $q$  ranging from 1.07 to 4.06 unitary charges have been reported (Mayer and Sugiyama, 1988; Cooper and Shrier, 1989; Greene, Haas, and Reiner, 1990; Fickler and Heinemann, 1992; Forsythe, Lindsell, and Stanfield, 1992). They are also larger than estimates of  $q$  for A-type currents in rabbit atrial cells and single smooth muscle cell of the guinea pig ureter, where values of  $\sim 2.5$  have been obtained (Clark et al., 1988; Imaizumi et al., 1990). The relatively large estimate of gating charge for  $I_A$  in AZF cells is, however, similar to that of *Drosophila* muscle A channels obtained from gating current measurements (Schoppa et al., 1992).

Half-maximal inactivation of  $I_A$  in AZF cells occurred at a membrane potential of  $-58.7$  mV. This is at least 10 mV more negative than the values obtained for  $I_A$  in other nonneuronal cells including heart, smooth muscle, and a pituitary cell line (Clark et al., 1988; Oxford and Wagoner, 1989; Imaizumi et al., 1990). Regardless, since the membrane potential of AZF cells is  $-71.1 \pm 1.1$  mV (Mlinar et al., 1993a), virtually all  $I_A$  channels would be available for activation in a resting cell. In contrast, the steady-state inactivation curves for mammalian neurons are shifted at least 20 mV in the hyperpolarizing direction compared with  $I_A$  current in AZF cells (Belluzzi et al., 1985; Mayer and Sugiyama, 1988; Greene et al., 1990; Forsythe et al., 1992). Most  $I_A$  current in many neurons is inactivated at the normal resting potential of these cells.

### Gating Kinetics

The sigmoidal onset kinetics of  $I_A$  in AZF cells were well described by single exponentials raised to integer powers of 4 or 5. Although the activation time constant was voltage dependent, it reached a minimum value at positive test potentials, indicating that both voltage-dependent and -independent transitions occur along the pathway from the closed to the open state. Systematic studies of activation kinetics of A currents in other vertebrate cells have not been reported. Therefore, it is not possible to conclude that the properties of  $I_A$  activation kinetics in AZF cells are common to rapidly inactivating  $K^+$  currents in other cells.

In early studies of  $I_A$  currents in *Gastropod* neurons, activation kinetics were modeled with Hodgkin-Huxley  $n^{3h}$  or  $n^{4h}$  formalisms. Activation time constants were either strongly voltage dependent (Neher, 1971) or voltage independent (Connor and Stevens, 1971).  $I_A$ 's in neurons and muscle cells of *Drosophila* also show this disparity in voltage dependence of activation kinetics (Solc, Zagotta, and Aldrich, 1987). It is likely that  $I_A$ -type channels will display considerable variation in activation kinetics just as they do in other biophysical properties and pharmacology.

$I_A$  in AZF cells inactivated with two time constants, both of which were voltage independent at test potentials ranging from  $-30$  to  $+40$  mV. These data indicate that open channels inactivate by mechanisms that are intrinsically voltage independent. In this regard, inactivation kinetics of  $I_A$  in AZF cells resemble voltage-gated  $Na^+$  and T-type  $Ca^{2+}$  currents and  $I_A$  currents in various cells, where inactivation rates have been reported to be independent of membrane potential (Clark et al., 1988; Akaïke, Kanaide, Kuga, Nakamura, Sadoshima, and Tomoike, 1989; Chen and Hess, 1990; Fickler and Heinemann, 1992). Inactivation may acquire an apparent voltage dependence when the voltage-dependent activation process becomes rate limiting in delivering channels to the open state. For most A currents, including those in AZF cells, activation kinetics are relatively fast over a wide range of potential. Consequently, inactivation occurs at a constant voltage-independent rate (Clark et al., 1988; Imaizumi et al., 1990; Fickler and Heinemann, 1992). However, voltage-dependent inactivation of a fast transient  $K^+$  current in sympathetic neurons has been reported (Belluzzi et al., 1985).

Although  $I_A$  currents in invertebrate neurons decay with single exponential time constants, inactivation kinetics of  $I_A$  are typically more complex in vertebrate cells. In dorsal root ganglion neurons and  $GH_4C_1$  pituitary cells, A-type currents inactivate with two time constants (Clark et al., 1988; Mayer and Sugiyama, 1988; Oxford and Wagoner, 1989).  $I_A$  in nodose neurons decays with three widely varying time constants, while single channel recordings identify only one type of  $I_A$  channel (Cooper and Shrier, 1989). Two pharmacologically separable A currents were coexpressed in a population of hypothalamic cells. Each of these inactivates with a single exponential time constant (Greene et al., 1990). Hippocampal neurons express, simultaneously, two A currents that inactivate with single and double exponential time constants (Fickler and Heinemann, 1992).

The complexity of  $I_A$  inactivation kinetics in many cells suggests that the "ball and chain model" which explains features of inactivation in *Drosophila* Shaker  $K^+$  channels (Hoshi, Zagotta, and Aldrich, 1990) will not be sufficient to explain

inactivation of all  $I_A$  currents. The spontaneous loss of  $I_A$  inactivation with time that we observed in AZF cells indicates that metabolic factors within the cell may modulate inactivation kinetics. Loss of inactivation of mammalian  $I_A$  currents expressed in *Xenopus* oocytes occurs through oxidation of cysteine residues on the NH<sub>2</sub>-terminal inactivation gate (Ruppersberg, Stocker, Pongs, Heinemann, Frank, and Koenen, 1991). Inactivation is restored by the reducing agent glutathione. The oxidizing agent chloramine-T slows inactivation of  $I_A$  current in rat hippocampal cells (Fickler and Heinemann, 1992). Thus,  $I_A$  channels in bovine AZF and other cells may be regulated physiologically by intracellular molecules that reduce or oxidize cysteine residues.

$I_A$  current in AZF cells recovered from inactivation by processes with two voltage-dependent time constants that differed greatly in magnitude. Although recovery kinetics of  $I_A$  currents in several cell types display clear voltage dependence (Belluzzi et al., 1985; Oxford and Wagoner, 1989; Imaizumi et al., 1990), few systematic studies of voltage-dependent recovery have been reported. In a number of cells where recovery has been studied at one or more potentials, the process can be described by a single exponential with a time constant resembling that of  $\tau_{\text{rec-f}}$  in AZF cells (Belluzzi et al., 1985; Imaizumi et al., 1990; Fickler and Heinemann, 1992). In neurons where  $I_A$  recovery occurs with two time constants, the slow time constant is an order of magnitude faster than that observed in AZF cells (Greene et al., 1990). Only in rabbit atrial and ventricular cells have recovery time constants comparable to  $\tau_{\text{rec-s}}$  in AZF cells been observed (Giles and Imaizumi, 1988).

In AZF cells, the slow but not the fast recovery time constant approached a voltage-independent minimum value at potentials near  $-80$  mV. Since 90% of  $I_A$  recovers with slow kinetics at the normal resting potential of AZF cells, full recovery of  $I_A$  current subsequent to inactivation would require at least 10 s. Since the normal electrical activity of AZF cells is not well understood, it is difficult to determine the impact of this long recovery period on cell physiology.

#### *Pharmacology*

With respect to block by organic antagonists, TEA and 4-AP,  $I_A$  in AZF cells resembled  $I_A$  in other cells. Observation of block after inactivation had been largely removed indicated that 4-AP effectively blocked A channels only after they had been opened by depolarization. 4-AP blocks K<sup>+</sup> current in lymphocytes with similar characteristics (Choquet and Korn, 1992).

$I_A$  was also reduced by the divalent cation Ni<sup>2+</sup>. Ni<sup>2+</sup> is well known as a selective blocker of T-type Ca<sup>2+</sup> channels. By comparison, Ni<sup>2+</sup> blocked T-type Ca<sup>2+</sup> channels in AZF cells 20 times more potently than A channels. Other divalent cations including Cd<sup>2+</sup> and Co<sup>2+</sup> have been reported to reduce  $I_A$  currents and to shift both steady-state activation and inactivation curves (Mayer and Sugiyama, 1988; Imaizumi et al., 1990). The trivalent cation La<sup>3+</sup> was at least one order of magnitude more potent than Ni<sup>2+</sup> at reducing  $I_A$  currents. La<sup>3+</sup> and other trivalents are also more potent than Ni<sup>2+</sup> and other divalents as antagonists of Ca<sup>2+</sup> channels, including T-type Ca<sup>2+</sup> channels found in AZF cells (Biagi and Enyeart, 1990, 1991; Mlinar et al., 1993b).

*Physiological Role*

Although  $I_A$  is a major current in AZF cells, its specific role in AZF function is unclear. In most neurons where  $I_A$  is present, this current acts as a frequency encoder spacing action potentials (Hille, 1992). With respect to voltage dependence of activation and steady-state inactivation,  $I_A$  in AZF cells more closely resembles A current in heart cells where  $I_A$  regulates repolarization and action potential duration (Giles and Imaizumi, 1988). Aside from  $I_A$  currents, the ion channels and electrical properties of neurons and cardiac myocytes are much different than those we have observed in AZF cells. Specifically, AZF cells possess no voltage-gated  $\text{Na}^+$  current and only T-type  $\text{Ca}^{2+}$  current. In intracellular recordings from >50 AZF cells at 37°C, we observed no spontaneous action potentials. Consequently,  $I_A$  may function differently in AZF cells than in other cells. In this regard, at the recorded resting potential of AZF cells (-71.1 mV),  $I_A$  and T-type  $\text{Ca}^{2+}$  channels are both available for activation by depolarization. The pituitary peptide adrenocorticotrophic hormone (ACTH) depolarizes these cells by inhibition of a distinct noninactivating  $\text{K}^+$  current which appears to set the resting potential of these cells (Mlinar et al., 1993a). ACTH did not inhibit either T- or A-type currents in bovine AZF cells. Under these conditions, the interplay between these two opposing transient currents would determine the membrane voltage, regulating  $\text{Ca}^{2+}$  entry and steroid hormone secretion.

This work was supported by National Institute of Diabetes and Digestive and Kidney grant DK-40131 to J. J. Enyeart.

*Original version received 17 August 1992 and accepted version received 13 April 1993.*

## REFERENCES

- Akaike, N., H. Kanaide, T. Kuga, M. Nakamura, J.-I. Sadoshima, and H. Tomoike. 1989. Low-voltage-activated calcium current in rat aorta smooth muscle cells in primary culture. *Journal of Physiology*. 416:141-160.
- Almers, W. 1978. Gating currents and charge movements in excitable membranes. *Review of Physiological and Biochemical Pharmacology*. 82:96-190.
- Belluzzi, O., O. Sacchi, and E. Wanke. 1985. A fast transient outward current in the rat sympathetic neurone studied under voltage-clamp conditions. *Journal of Physiology*. 358:91-108.
- Biagi, B. A., and J. J. Enyeart. 1990. Gadolinium blocks low- and high-threshold calcium currents in pituitary cells. *American Journal of Physiology*. 259:C515-C520.
- Biagi, B. A., and J. J. Enyeart. 1991. Multiple calcium currents in a thyroid C-cell line: biophysical properties and pharmacology. *American Journal of Physiology*. 260:C1253-C1263.
- Brauneis, U., P. M. Vassilev, S. J. Quinn, G. H. Williams, and D. L. Tillotson. 1991. ANG II blocks potassium currents in zona glomerulosa cells from rat, bovine and human adrenals. *American Journal of Physiology*. 260:E772-E779.
- Chen, C., and P. Hess. 1990. Mechanisms of gating of T-type calcium channels. *Journal of General Physiology*. 96:603-630.
- Choquet, D., and H. Korn. 1992. Mechanism of 4-aminopyridine action on voltage-gated potassium channels in lymphocytes. *Journal of General Physiology*. 99:217-240.
- Clark, R. B., W. R. Giles, and Y. Imaizumi. 1988. Properties of the transient outward current in rabbit atrial cells. *Journal of Physiology*. 405:147-168.



- Connor, J. A., and C. F. Stevens. 1971. Voltage clamp studies of a transient outward membrane current in gastropod neural somata. *Journal of Physiology*. 213:21–30.
- Cooper, E., and A. Shrier. 1989. Inactivation of A currents and A channels on rat nodose neurons in culture. *Journal of General Physiology*. 94:881–910.
- Fickler, E., and U. Heinemann. 1992. Slow and fast transient potassium currents in cultured rat hippocampal cells. *Journal of Physiology*. 445:431–455.
- Forsythe, I. D., P. Linsdell, and P. R. Stanfield. 1992. Unitary A-currents of rat locus coeruleus neurones grown in cell culture: rectification caused by internal Mg<sup>2+</sup> and Na<sup>+</sup>. *Journal of Physiology*. 451:553–583.
- Giles, W. R., and Y. Imaizumi. 1988. Comparison of potassium currents in rabbit atrial and ventricular cells. *Journal of Physiology*. 405:123–145.
- Greene, R. W., H. L. Haas, and P. B. Reiner. 1990. Two transient outward currents in histamine neurones of the rat hypothalamus *in vitro*. *Journal of Physiology*. 420:149–163.
- Halliwel, J. V., I. B. Othman, A. Pelchen-Matthews, and J. O. Dolly. 1986. Central action of dendrotoxin: selective reduction of a transient K<sup>+</sup> conductance in hippocampus and binding to localized receptors. *Proceedings of the National Academy of Sciences, USA*. 83:493–497.
- Hille, B. 1992. *Ionic Channels of Excitable Membranes*. Sinauer Associates, Inc., Sunderland, MA. 607 pp.
- Hoshi, T., W. N. Zagotta, and R. W. Aldrich. 1990. Biophysical and molecular mechanisms of Shaker potassium channel inactivation. *Science*. 250:533–538.
- Imaizumi, Y., K. Muraki, and M. Watanabe. 1990. Characteristics of transient outward currents in single smooth muscle cells from the ureter of the guinea-pig. *Journal of Physiology*. 427:301–324.
- Lymangrover, J. R., E. K. Matthews, and M. Saffran. 1982. Membrane potential changes of mouse adrenal zona fasciculata cells in response to adrenocorticotropin and adenosine 3',5'-monophosphate. *Endocrinology*. 110:462–468.
- MacKinnon, R. 1991. Determination of the subunit stoichiometry of a voltage-activated potassium channel. *Nature*. 350:232–235.
- Mayer, M. L., and K. Sugiyama. 1988. A modulatory action of divalent cations on transient outward current in cultured rat sensory neurones. *Journal of Physiology*. 396:417–433.
- Mlinar, B., B. A. Biagi, and J. J. Enyeart. 1993a. A novel K<sup>+</sup> current inhibited by ACTH and Angiotensin II in adrenal cortical cells. *Journal of Biological Chemistry*. 268:8640–8644.
- Mlinar, B., B. A. Biagi, and J. J. Enyeart. 1993b. Voltage-gated transient currents in bovine adrenal fasciculata cells. I. T-type Ca<sup>2+</sup> current. *Journal of General Physiology*. 101:217–237.
- Neher, E. 1971. Two fast transient current components during voltage clamp on snail neurons. *Journal of General Physiology*. 58:36–53.
- Oxford, G. S., and P. K. Wagoner. 1989. The inactivating K<sup>+</sup> current in GH<sub>3</sub> pituitary cells and its modification by chemical reagents. *Journal of Physiology*. 410:587–612.
- Quinn, S. J., M. C. Cornwall, and G. H. Williams. 1987. Electrical properties of isolated rat adrenal glomerulosa and fasciculata cells. *Endocrinology*. 120:903–914.
- Ruppersberg, J. P., M. Stocker, O. Pongs, S. H. Heinemann, R. Frank, and M. Koenen. 1991. Regulation of fast inactivation of clones mammalian I<sub>K(A)</sub> channels by cysteine oxidation. *Nature*. 352:711–714.
- Schoppa, N. E., K. McCormack, M. A. Tanouye, and F. J. Sigworth. 1992. The size of gating charge in wild-type and mutant Shaker potassium channels. *Science*. 255:1712–1715.
- Solc, C. K., W. N. Zagotta, and R. W. Aldrich. 1987. Single-channel and genetic analyses reveal two distinct A-type potassium channels in *Drosophila*. *Science*. 236:1094–1098.